

Design of A New Probe for Tumor Treatment in the Alternate Thermal System Based on Numerical Simulation

Zhanghao Cai, Mingyang Song, Jianqi Sun*, Aili Zhang, Lisa X. Xu*

School of Biomedical Engineering and Med-X Research Institute, Shanghai Jiao Tong University, P. R. China

*Corresponding E-mail Address: milesun@sjtu.edu.cn, lisaxu@sjtu.edu.cn

Abstract— A new probe for tumor treatment is designed and simulated in this study. This probe combines the cryosurgery and hyperthermia which is suitable for the treatment of subcutaneous tumors. Simulations of the cooling and heating processes demonstrate that the probes are capable of treating the tumor effectively. And the numerical results indicate that the lengths of the probe, the diameters of the inner tube and the pressures of liquid nitrogen influence the probes' cooling ability. The temperature responses at the tumor base induced by different probes are similar, though the great differences appear on the treatment interface of the probes, thus the temperature gradient within the tumor. Based on the simulation results, the heating effect of the probe is shown to be effective in damaging the tumor while protecting normal tissue in the surrounding. Animal experiments will be carried out using this type of probe to treat tumor in the near future.

I. INTRODUCTION

Thermophysical treatment is an efficient therapy for tumors, aiming at demolishing the target tumor through an ablation with extremely low or high temperature. In the mid-1960, Cooper began the modern cryosurgery and improved the techniques [1]. Compared to the conventional clinical modalities, cryosurgery has obvious advantages, such as fewer bleeding, anesthetic effect during the cryogenic producer, little destruction on normal tissues, and so on [2]. Early reports focused on one technical aspects of cryosurgery, i.e. how to accelerate the efficiency of freezing. Basic features of the cryosurgical technique were proposed, i.e. rapid freezing, slow thawing, repetition of the freezing-thaw cycles [1, 3]. Recently, a new theory has become appealing that cryogenic therapy may induce the immunologic responses [4-11].

Radiofrequency (RF) is another method used to ablate tumor tissue efficiently, which has been widely used clinically and implemented as commercial products. Physicians have applied this technique to treat many kinds of tumors such as skin, gastrointestinal, tracheobronchial and intracranial tumors [12].

Combination of cooling and heating therapy has been developed recently. One type is composed of cryogen evaporation for cooling, and RF for heating. The other is based on Joule-Thomson effect of Argon gas or Nitrogen gas [2, 13].

Sun et al. designed and developed an alternate cooling and heating system. Experiments were performed in the VX2 breast carcinoma model in female New Zealand rabbits [14]. They demonstrated that no metastasis and recurrence appeared in the following three months after such alternate cooling and heating treatment. A new experiment about thermal physical method combining both cryosurgery and local hyperthermia was used to treat mice bearing 4T1 murine mammary carcinoma by Dong et al. [15]. The results suggested that alternate cooling and heating had synergistic effect and resulted in the stimulation of whole body immune response. The second challenges of tumors in the treated mice were rejected. Liu et al. also developed a cryoprobe system with a steam heating device. They revealed the thermal stress mechanisms in tissues. But this system was only based on conduction heat transfer, less effective in thermal penetration [16]. Takahashi built the treatment system integrating cryosurgery and hyperthermia [13]. They concluded that combination treatment of both was effective to destroy the tissue and the higher temperature applied immediately after thawing in cryosurgery might reinforce the tissue destruction.

In this study, a probe suitable for treating subcutaneous tumors in particular based on LN₂ cryosurgery and RF hyperthermia is designed and studied. The cycle of cooling by liquid nitrogen and heating by RF is found to enhance the efficiency of thermo-physical therapy for subcutaneous tumors.

II. PROBE DESIGN AND HEAT ANALYSIS

A. Probe design

The design of probe is shown in figure 1. The device is consisted of five parts: inner tube, out tube, treatment interface, exhausting pipe and T type pipe. There are three types of probes. Probe 1 is 70mm long and the diameter of inner tube is 1mm; probe 2 is 100mm long and 1.5mm in diameter; and probe 3 is 100mm long and 2mm in diameter; The treatment interface is round with a diameter about 10mm. An inner tube is inserted in the probe with a certain distance from the treatment interface, no more than 2mm. The diameter of probe wall is 5mm. During cooling, the liquid nitrogen flows out from a Dewar, and flows into inner tube(1), then jets at the treatment interface(3), causing the interface to cool down to a controlled aim temperature at last. Then after heat exchanging, the fluid flows out of the tube and T type pipe (5) through the exhausting pipe (4). The temperature of the treatment interface can finally get to the range of -160°C and -175°C, according to different inner

This work was supported by National Natural Science Foundation of China (NSFC11005074, NSFC50725622), Doctoral Fund of Ministry of Education of China (20100073120004), and National Basic Research Program of China (973 Program, 2010CB834300).

tubes. Not only is the treatment interface used as cryogenic unit but also severed as an electrode when RF is generated. The interface is quite fit to the size of subcutaneous tumors in our 4T1 tumor model of mice. The ground electrode is located under the body.

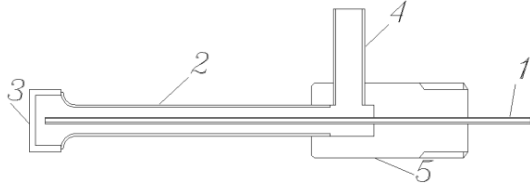


Fig.1 Design of the probe.
1, inner tube, 2, out tube, 3, treatment interface, 4, exhausting pipe, 5, T type pipe

B. Thermal analysis

The probe is directly pressed to the skin where tumor grows inside. Then cooling and heating treatment can be performed alternately by this probe.

A numerical model has been established by Gambit to simulate the performance of the probe. The finite volume method (FVM) based model is calculated by FLUENT. There are three parts in the model: probe, tumor and normal tissues. Tumor and tissue are assumed to be symmetric to the axis, so the model can be simply designed as two-dimensional axi-symmetric shapes as shown in figure 2. The tumor in the model is 5mm wide which is half of the whole tumor, and its thickness is 7mm. The size of tissue is 20 mm × 14mm.

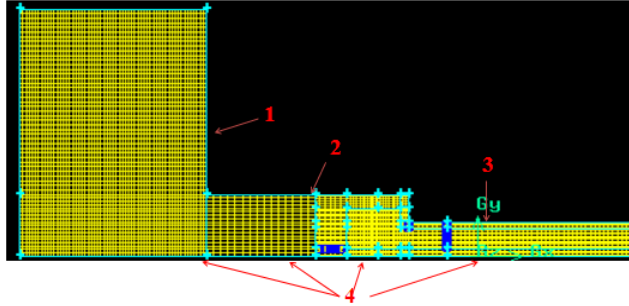


Fig.2 1-tissue, 2-tumor, 3-probe, 4-axis

In the FVM calculation, Mixture Model is used to simulate flowing and heat transfer of liquid nitrogen and nitrogen gas in the probe. In the Mixture Model, continuity equation, momentum equation and energy equation need to be solved for the mixture.

The continuity equation is shown as:

$$\frac{\partial}{\partial t}(\rho_m) + \nabla \cdot (\rho_m \vec{v}_m) = 0 \quad (1)$$

where \vec{v}_m is the mass-averaged velocity, ρ_m is the mixture density.

The momentum equation for the mixture summing all phases momentum equations can be expressed as:

$$\frac{\partial}{\partial t}(\rho_m \vec{v}_m) + \nabla \cdot (\rho_m \vec{v}_m \vec{v}_m) = -\nabla p + \nabla \cdot [\mu_m (\nabla \vec{v}_m + \nabla \vec{v}_m^T)] + \rho_m \vec{g} + \vec{F} + \nabla \cdot \left(\sum_{k=1}^n a_k \rho_k \vec{v}_{dr,k} \vec{v}_{dr,k} \right) \quad (2)$$

where n is the number of phases, which is 2 here; \vec{F} is the body force, and \vec{v}_m is the viscosity of the mixture; $\vec{v}_{dr,k}$ is the drift velocity for secondary phase, and is 0 here.

The energy equation for the mixture takes the following form:

$$\frac{\partial}{\partial t} \sum_{k=1}^n (a_k \rho_k E_k) + \nabla \cdot \sum_{k=1}^n (a_k \vec{v}_k (\rho_k E_k + p)) = \nabla \cdot (k_{eff} \nabla T) + S_E \quad (3)$$

where k_{eff} is the effective conductivity, the first term on the right side of equation is energy transfer due to conduction. S_E includes any other volumetric heat sources. $E_k = h_k$ for an incompressible phase and h_k is the sensible enthalpy.

The Pennes equation [17] is used as the governing equation for heat transfer in both tumor and tissue:

$$\rho_t C_p \frac{\partial T}{\partial t} = \nabla \cdot (k \nabla T) + \rho_b c_b w_b (T_a - T_t) + Q_{met} \quad (4)$$

where ρ_t is tissue's density (kg/m^3), C_p is specific heat of tissues ($\text{J}/\text{kg} \cdot ^\circ\text{C}$), ρ_b is the density of blood and c_b is specific heat of blood, w_b is the blood perfusion rate, Q_{met} is the volumetric metabolic heat, and here is neglected.

To obtain the heating effects of the probe on the tissue, the specific absorption rate (SAR) is calculated in the software (COMSOL) based on the finite element method (FEM). In the tissue, the lower frequency is corresponding to a longer wavelength [18]. And Electromagnetic fields can be regarded as quasi-stationary state field. So by simply mathematical derivations, we obtain [19]:

$$\nabla \cdot [\sigma(T) \nabla V] = 0 \quad (5)$$

where V is the electrical potential (V) and T is the temperature ($^\circ\text{C}$). The thermal performance is governed by the bio-heat equation:

$$\rho_t C_p \frac{\partial T}{\partial t} = \nabla \cdot (k \nabla T) + \rho_b c_b w_b (T_a - T_t) + Q_{met} + q \quad (6)$$

The added q is the electrical energy source. That is calculated by COMSOL to convert the electromagnetic energy to heat.

The simulation of heating on the tumor with RF is also two-dimensional axi-symmetric like the cooling model. The thickness of tumor is 7mm, and 5mm wide. The frequency of RF is 460 kHz, and the voltage is accelerated slowly to 20V.

The parameters of the tumors and muscle tissues are cited in the table 1 [19].

TABLE 1
ELECTICAL AND THERMAL PARAMETERS

type	Electric conductivity (S/m)	Thermal conductivity (W/(m·°C))	Specific heat (kJ/(kg·°C))	Density (kg/m ³)
tumor	0.64	0.56	3689	1050
muscle	0.64	0.56	3639	1050

III. RESULTS AND DISCUSSION

In the experiment of cooling, the temperature at the tumor base in conjunction to normal tissue is cooled to 273K in 2 minutes and kept for 5 minutes through feedback control algorithm. Then a RF power is induced to heat the tumor to 318K after about ten minutes natural thawing. The temperature has been monitored and controlled through the whole process which will not exceed the desired value.

Figure 3 shows the processes of freezing in 2 minutes on the treatment interfaces of different probes. Shown in this figure, probe 3 has the greatest freezing ability. That is because its inner tube is wider than that of probe 2 and probe 1. The radius of inner tube is considered as the primary factor influencing the freezing ability of probes. The large inner tube in diameter allows for much more liquid nitrogen flowing into the probe than smaller ones. More mass flux would be benefit for cooling. Although probe 2 is longer than probe 1, its larger inner tube enhances its cooling rate.

In figure 4, the processes of cooling with different pressures are simulated for probe 2. The blue, red and green lines represent the processed of cooling with 3, 5 and 7 standard atmospheric pressures, respectively. It is shown that when the inlet pressure is higher, the final temperature on the treatment interface is lower due to larger heat convection by higher flow velocity under higher pressure.

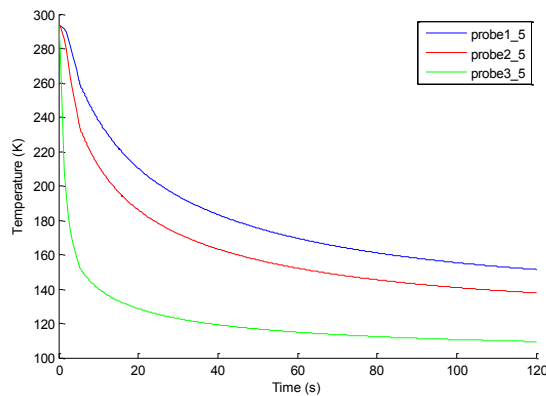


Fig.3 The processes of cooling down about probe 1, 2, 3 are simulated under 5 standard atmospheric pressure. The blue line represents process of freezing of probe 1; the red line represents process of freezing of probe 2; the green line represents process of freezing of probe 3.

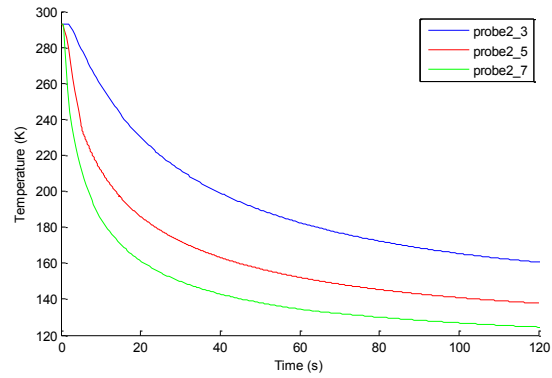


Fig.4 The processes of cooling down about probe 2 are simulated under 3, 5, 7 standard atmospheric pressures respectively. The blue line represents process of freezing under 3 standard atmospheric pressures; the red line represents process of freezing under 5 standard atmospheric pressures; The green line represents process of freezing under 7 standard atmospheric pressures.

The different velocities under different pressures at the outside of inner tube are shown in table 2. The higher the pressure, the larger the velocity is. The variations of velocities greatly affect the cooling ability of the probes.

TABLE 2
VELOCITY OF THREE TYPEs OF PROBES UNDER DIFFERENT PRESSURES

Probe type	Velocity under 3 sap ^a (m/s)	Velocity under 5 sap (m/s)	Velocity under 7 sap (m/s)
Probe1	20.11	29.06	35.85
Probe2	17.57	25.08	31.51
Probe3	19.33	26.55	32.81

^asap is abbreviation of standard atmospheric pressures

In figure 5, the temperature mapping after freezing for 2 minutes is shown. Near the treatment interface, the temperature of the tissue is almost equal to that of probe. And there is a large temperature gradient within the tumor. The temperature at the tumor base in conjunction to normal tissue is about 273K, caused by the thermal resistance thru tissue.

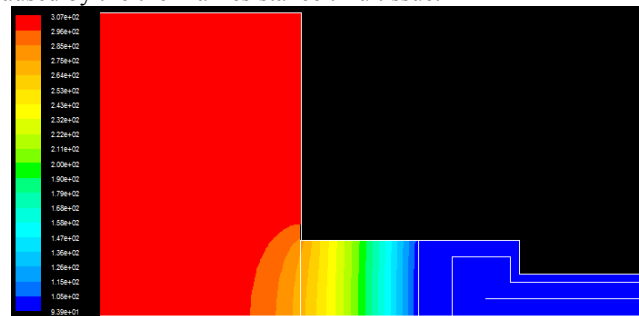


Fig.5 Contour of temperature for freezing for 2 min of probe 3 under 5 standard atmospheric pressure

The result shown in figure 6 is a process simulated by COMSOL about the heating of RF in 5 minutes. The temperature rise becomes less steep along with the time, and it takes about 2 minutes to reach 318K, whose distribution is shown in figure 7. In the simulation, the tumor temperature is raised higher than 318K while less heating occurs in normal tissue. And the edge temperature is lower than the center in tissue because of the air convection.

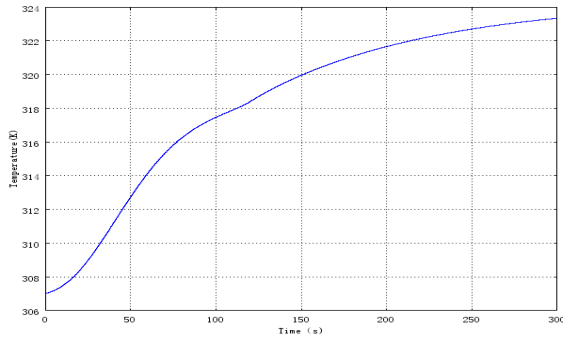


Fig.6 The temperature on the border between the tumor and tissues during RF heating in 5 minutes

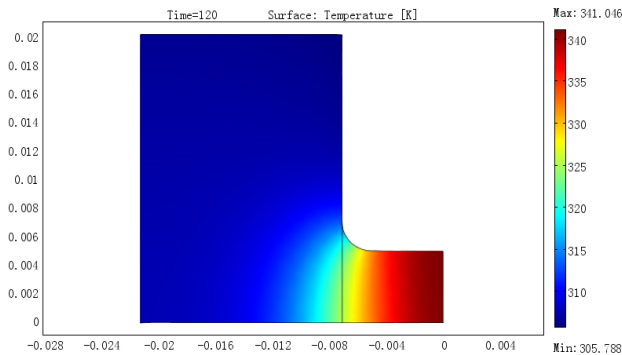


Fig.7 The distribution of temperature by heating the tumor

IV. CONCLUSION

In this study, a new probe has been designed which can perform cryosurgery and hyperthermia for treating subcutaneous tumors. Simulation results show that the length of the tube, the diameter of the inner tube and the pressures all have effects on the freezing ability of the probe. With the pressure of 7 standard atmospheric pressures in the probe 3, the ability of freezing is better than other configurations. The heating process proves that the probe can heat the tumor quickly while keeping the normal tissues intact through a feedback control algorithm. Experiments in the animal tissues both in vitro and in vivo will be performed to further test the performance of the probe.

REFERENCES

- [1] A. A. Gage, and J. Baust, *Mechanisms of Tissue Injury in Cryosurgery*. Cryobiology, 1998. 37(3): p. 171-186
- [2] J. Q. Sun, A. L. Zhang, and L. X. Xu, *Evaluation of alternate cooling and heating for tumor treatment*. International Journal of Heat and Mass Transfer, 2008, p.5478-5485
- [3] A. A. Gage, *Selective cryotherapy*. Cell Preservation Technology, 2004. 2(1): p. 3-14.
- [4] N. E. Hoffmann, and J. C. Bischof, *The cryobiology of cryosurgical injury*. Urology, 2002. 60(2A): p. 40-49.J.
- [5] H. Neel III, A. Ketcham, and W. Hammond, *Experimental evaluation of in situ oncoide for primary tumor therapy: Comparison of tumor-specific immunity after complete excision, cryonecrosis and ligation*. The Laryngoscope, 1973. 83(3): p. 376-387
- [6] H. Neel III, and R. Ritts Jr, *Immunotherapeutic effect of tumor necrosis after cryosurgery, electrocoagulation, and ligation*. Journal of surgical oncology, 1979. 11(1): p. 45.
- [7] K. Miya, S. Saji, T. Morita, H. Niwa, H. Takao, H. Kida and K. Sakata, *Immunological response of regional lymph nodes after tumor cryosurgery: experimental study in rats*. Cryobiology, 1986. 23(4): p. 290-295.
- [8] K. Washington, J. P. Debelak, C. Gobbell, D. Sztipanovits, Y. Shyr, S. Olson and W. C. Chapman, *Hepatic cryoablation-induced acute lung injury: histopathologic findings*. Journal of Surgical Research, 2001. 95(1): p. 1-7.
- [9] J. K. Seifert, M. P. France, J. Zhao, E. J. Bolton, I. Finlay, T. Junginger, and D. L. Morris, *Large volume hepatic freezing: association with significant release of the cytokines interleukin-6 and tumor necrosis factor α in a rat model*. World journal of surgery, 2002. 26(11): p. 1333-1341
- [10] A. L. Zhang, L. X. Xu, G. A. Sandison, and J. Zhang, *A microscale model for prediction of breast cancer cell damage during cryosurgery*. Cryobiology, 2003. 47(2): p. 143-154.
- [11] A. A. Gage, J. M. Baust, and J. G. Baust, *Experimental cryosurgery investigations in vivo*. Cryobiology, 2009. 59(3): p. 229-243.
- [12] Y. Ni, S. Mulier, Y. Miao, L. Michel, and G. Marchal, *A review of the general aspects of radiofrequency ablation*. Abdominal imaging, 2005. 30(4): p. 381-400.
- [13] D. Takahashi, T. Takahashi, K. Sone, and I. Fukumoto, *A Study for Cryosurgery-Hyperthermia Treatment System*. Journal of Power and Energy Systems, 2008. 2(5): p. 1294-1303.
- [14] J. Q. Sun, C. C. Xu, G. H. Wei, X. G. Sun, P. Liu, A. L. Zhang and L. X. Xu, "Tumor Treatment System with Alternate Cooling and Heating-Preliminary Results in an Animal Model," World Congress On Medical Physics And Biomedical Engineering, September 7, 2009, to be published.
- [15] J. Dong, P. Liu, and L. X. Xu, *Immunologic response induced by synergistic effect of alternating cooling and heating of breast cancer*. International Journal of Hyperthermia, 2009. 25(1): p. 25-33.
- [16] J. Liu, Y. Zhou, T. Yu, and L. Gui, *Minimally invasive probe system capable of performing both cryosurgery and hyperthermia treatment on target tumor in deep tissues*. Minimally Invasive Therapy and Allied Technologies, 2004. 13(1): p. 47-57.
- [17] H. Pennes, *Analysis of tissue and arterial blood temperatures in the resting human forearm*. Journal of applied physiology, 1948. 1(2): p. 93.
- [18] V. D'Ambrosio and F. Dughier, *Numerical model for RF capacitive regional deep hyperthermia in pelvic tumors*. Medical and Biological Engineering and Computing, 2007. 45(5): p. 459-466.
- [19] E. Vilhelm, W. Hans, and E. Anders, *Influence of electrical and thermal properties on RF ablation of breast cancer: is the tumour preferentially heated?* BioMedical Engineering OnLine, 2005. 4(1): p. 41.